Radiative energy loss and v_2 spectra for viscous hydrodynamics

Kevin Dusling,[1] Guy D. Moore,[2] and Derek Teaney[3]

[1]*Physics Department, Building 510A, Brookhaven National Laboratory, Upton, New York 11973, USA*
[2]*Department of Physics, McGill University, 3600 rue University, Montréal, Quebec H3A 2T8, Canada*
[3]*Department of Physics and Astronomy, Stony Brook University, Stony Brook, New York 11794, USA*

This work investigates the first correction to the equilibrium phase-space distribution and its effects on spectra and elliptic flow in heavy-ion collisions. We show that the departure from equilibrium on the freeze-out surface is the largest part of the viscous corrections to $v_2(p_T)$. However, the momentum dependence of the departure from equilibrium is not known *a priori*, and it is probably not proportional to p_T^2 as has been assumed in hydrodynamic simulations. At high momentum in weakly coupled plasmas, it is determined by the rate of radiative energy loss and is proportional to $p_T^{3/2}$. The weaker p_T dependence leads to straighter $v_2(p_T)$ curves at the same value of viscosity. Furthermore, the departure from equilibrium is generally species dependent. A species-dependent equilibration rate, with baryons equilibrating faster than mesons, can explain "constituent quark scaling" without invoking coalescence models.

I. INTRODUCTION

When two ultrarelativistic nuclei collide, they leave behind a region of high energy-density QCD matter, whose properties we would like to understand better. The initial geometry of the QCD matter is set by the overlap region of the two colliding nuclei. Generally, the nuclei collide at finite impact parameter rather than head-on. In this case, the initial geometry is not a disk, but is an "almond-shaped" ellipse. (The short and long axis of the initial almond are taken as the x and y axes, respectively.) The production mechanism of the QCD matter is local and knows nothing of this global geometry. Therefore, to a first approximation the initial stress tensor will be locally azimuthally symmetric. Subsequently, if there are no reinteractions, the produced matter will free stream to the detector; the initial geometry will have no influence on the evolution, and the angular distribution of the final observed hadrons will also be azimuthally symmetric. On the other hand, if there are strong interactions which maintain local thermal equilibrium, the pressure gradients in the x direction will be larger than in the y direction, an anisotropy in the collective flow will develop, and ultimately an anisotropy in the momentum spectrum of the final hadrons will be observed.

The final momentum anisotropy is characterized experimentally by v_2, the second harmonic of the azimuthal distribution of the produced particles with respect to the reaction plane. Experimentalists have measured v_2 as a function of transverse momentum p_T, particle type, and impact parameter [1–4]. These results are surprisingly well described by ideal hydrodynamics [5], which amounts to the approximation that the interactions are fast enough to maintain the matter in equilibrium from an early time until hadronic freeze-out. There are some limits to this success. First, the measured v_2 falls below the ideal hydrodynamic prediction for momenta larger than $p_T \gtrsim 2.0$ GeV. Second, the hydrodynamic fit fails to reproduce certain relative trends observed in the baryon and meson elliptic flows. These trends are compactly summarized by "constituent quark scaling" [6–8] which generally has been attributed to a kind of coalescence of constituent quarks [9–12]. Here we will argue that the first corrections to equilibrium can clarify both of these shortcomings without the need for a coalescence model.

To quantify the corrections to ideal hydrodynamics, it is important to study nonideal (viscous) hydrodynamics. In the last 2 years, there has been a major push in this direction [13–20]. These studies have used various formalisms and have studied variations of $v_2(p_T)$ with respect to the input shear viscosity, the model for the initial geometry, and various other nuisance parameters. However, we want to point out here that these studies have all made a common assumption about the way that the asymmetry in the stress tensor is manifested in the particle distribution after freeze-out. In particular, the particle distribution after freeze-out is locally of the form $f = f_0 + \delta f$, where f_0 is the equilibrium distribution and δf is the first correction. All groups have assumed that $\delta f(p) \propto p^2 f_0$ and that the coefficient of proportionality is independent of particle type.

In this paper, we will argue that this assumption matters, and that it is far from secure. After an overview of the issue in the next section, in Sec. III we will discuss the physics that establishes the momentum dependence of δf and its behavior in several theories. We will see that while the most studied theories give $\delta f \propto p^2 f_0$, the most QCD-like theories do not. Then we explore the behavior of multicomponent plasmas in Sec. IV. We see there that the viscous corrections $\delta f(p)$ for different species are generically different. This fact can account for the "constituent quark scaling" observed in the baryon and meson elliptic flows without any reference to the hadronization process. We then make our concluding remarks. Some technical material is postponed to appendixes.

Throughout, we will denote four-vectors with capital letters P, Q and use $\boldsymbol{p}$, $\boldsymbol{q}$ for their three-vector components, E_p, E_q for their energy components, and p, q for $|\boldsymbol{p}|$, $|\boldsymbol{q}|$. Our metric convention is $[-, +, +, +]$, so that $u_\mu u^\mu = -1$. We use tilde to indicate momenta scaled by temperature, $\tilde{p} \equiv p/T$.

We will mostly write n_p for the equilibrium distribution function, $n_p \equiv 1/[\exp(p/T) \mp 1]$, but will occasionally use $f_0(p)$ when common convention dictates its use. The appropriate statistics will be clear from the context.

II. OVERVIEW

The energy momentum tensor is given by the sum of its ideal and dissipative parts,[1]

$$T^{\mu\nu} = (\epsilon + \mathcal{P})u^\mu u^\nu + \mathcal{P}g^{\mu\nu} + \pi^{\mu\nu}, \qquad (1)$$

and obeys the equation of motion,

$$\partial_\mu T^{\mu\nu} = 0. \qquad (2)$$

In the first-order (or Navier-Stokes) approximation, the dissipative part of the stress energy tensor in the local rest frame is

$$\pi^{ij} = -\eta\left(\partial^i u^j + \partial^j u^i - \tfrac{2}{3}\delta^{ij}\partial_k u^k\right)$$
$$\equiv -\eta\sigma^{ij} \equiv -2\eta\langle\partial^i u^j\rangle, \qquad (3)$$

where η is the shear viscosity, and we use $\langle\cdots\rangle$ to indicate that the bracketed tensor should be symmetrized and made traceless. It is well known that the first-order theory is plagued with difficulties such as causality violations and instabilities [21,22]. To circumvent these issues, a second-order theory is required. The most commonly used second-order relativistic viscous hydrodynamics is that from Israel and Stewart [23]. For technical reasons, we use a theory developed by Öttinger and Grmela [24,25]. The two theories are qualitatively the same (i.e., for sufficiently small relaxation times, they both approach the first-order theory). To streamline the presentation, we postpone the details of our hydrodynamic model to Appendix A and refer to previous work [17].

The solutions to the hydrodynamic equations yield the underlying temperature and flow profiles in the presence of viscosity. Particle spectra are then computed using the Cooper-Frye [26] formula

$$E\frac{d^3 N}{d^3 p} = \frac{\nu}{(2\pi)^3}\int_\sigma f(\tilde{p})p^\mu d\sigma_\mu, \qquad (4)$$

where $\tilde{p} \equiv p/T$ and σ_μ is the freeze-out hypersurface taken as a surface of constant energy density in this work. For a system out of equilibrium, $f(\tilde{p})$ is not the equilibrium distribution function but also contains viscous corrections,

$$f(\tilde{p}) = f_0(\tilde{p}) + \delta f(\tilde{p}), \qquad (5)$$

where f_0 is the ideal Bose/Fermi distribution function. The form of δf is constrained by the requirement that T^{ij} be continuous across the freeze-out hypersurface:

$$T^{\mu\nu} = \nu\int\frac{d^3 p}{(2\pi)^3 p^0}p^\mu p^\nu f(\tilde{p}) \quad\rightarrow$$

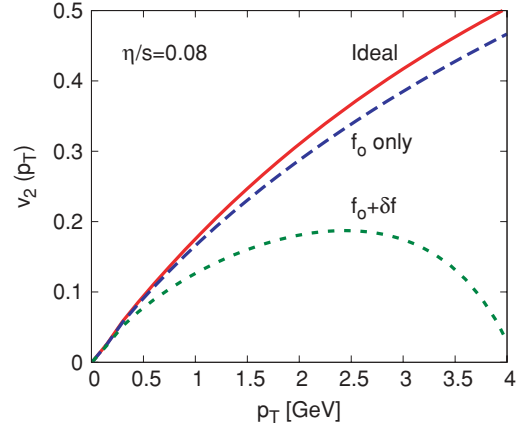$$\pi^{ij} = \nu\int\frac{d^3 p}{(2\pi)^3 p^0}p^i p^j \delta f(\tilde{p}). \qquad (6)$$

FIG. 1. (Color online) Typical results for $v_2(p_T)$ from a viscous hydrodynamic model employing the quadratic *Ansatz*. The run parameters are $\eta/s = 0.08$, $T_{\text{frzout}} = 140$ MeV, and $p = 1/3\epsilon$. Further details are in Appendix A.

Dropping δf from the final particle spectra is inconsistent, because it leads to a discontinuity in $T^{\mu\nu}$. The form for δf which satisfies continuity in the local rest frame is proportional to $\hat{p}^i \hat{p}^j \pi_{ij}$ and is traditionally parametrized by $\chi(p)$ as[2]

$$\delta f(\boldsymbol{p}) = -n_p(1 \pm n_p)\chi(\boldsymbol{p}), \qquad (7)$$

$$= -\chi(p)n_p(1 \pm n_p)\hat{p}^i \hat{p}^j\langle\partial_i u_j\rangle, \qquad (8)$$

where we have distinguished $\chi(p)$ and $\chi(\boldsymbol{p}) \equiv \chi(p)\hat{p}^i \hat{p}^j\langle\partial_i u_j\rangle$ by the argument of the function. One moment of $\chi(p)$ is fixed by the shear viscosity (see below) but otherwise $\chi(p)$ is an arbitrary function of p. To date, all works on viscous hydrodynamics have taken the quadratic *Ansatz* and have usually worked in a Boltzmann approximation

$$\chi(p) \propto p^2. \qquad (9)$$

Let us look at typical results for $v_2(p_T)$ as shown in Fig. 1. The curve labeled 'Ideal' shows the result using ideal hydrodynamics (i.e., $\eta/s = 10^{-6}$). The curve labeled 'f_0' shows the resulting elliptic flow from the viscous evolution [the solution of Eqs. (2), (3), and (A2)] but without including the viscous correction to the distribution function. In other words, this shows how the viscous correction to the temperature and flow profiles manifests itself in the particle spectra. Only modest corrections to the spectra are found. As already emphasized, this result is unphysical, since dropping δf violates continuity of the stress tensor. Last, the curve labeled '$f_0 + \delta f$' also takes δf into account, using the quadratic *Ansatz*. The viscous correction to the distribution function dominates the reduction in v_2 at large p_T. That means that the δf term is responsible for a significant part of the effects of viscosity in the particle spectra.

---

[1]We use Landau-Lifshitz conventions to fix ϵ, u^μ in terms of four components of $T^{\mu\nu}$. The other six independent components of $T^{\mu\nu}$ can always be accommodated by a $\pi^{\mu\nu}$ satisfying $u_\mu\pi^{\mu\nu} = 0$.

[2]In actual simulations, π^{ij} is treated as a dynamical variable in a second-order fluid formalism. Then to first order, one can make the replacement, $\langle\partial_i u_j\rangle \rightarrow -\pi_{ij}/2\eta$. There has been no attempt to systematically include δf through second order in hydrodynamic simulations.

This being the case, it is imperative to perform a systematic study on the form of the viscous correction as well as its effect on elliptic flow. Most of this paper will discuss the form of the viscous correction appearing in weakly coupled QCD. Although this is not a theory of hadronizing QCD, it is one theory where quantitative first-principle calculations can be performed. One of our major findings is that not all models of energy loss give the same predictions for the off-equilibrium distribution function.

III. FORM OF δf IN SEVERAL THEORIES

In this section, we consider a number of theories, to show that while the dependence $\chi(p) \propto p^2$ is expected in some cases, other functional dependence is expected in others, including weakly coupled QCD and a hadron (resonance) gas. The theories where we can make a definite statement about the functional form of δf are all described by kinetic theory. Since freeze-out is defined as the point where scatterings go from being common to being rare on the time scale of the evolution of the system, we generally expect that *just* before freeze-out, kinetic theory should be a reasonable description.

Within kinetic theory, the distribution function $f(\boldsymbol{p}, \boldsymbol{x})$ is determined by a Boltzmann equation,

$$(\partial_t + v_{\mathbf{p}} \cdot \partial_{\mathbf{x}}) f(\boldsymbol{p}, \boldsymbol{x}) = -\mathrm{C}[f, \boldsymbol{p}], \qquad (10)$$

where $\mathrm{C}[f, \boldsymbol{p}]$ is the collision operator. In equilibrium, the distribution function obeys

$$n(\boldsymbol{p}, \boldsymbol{x}) = \frac{1}{e^{-P_\mu u^\mu(t, \boldsymbol{x})/T(t, x)} \mp 1}, \quad \text{with} \quad \mathrm{C}[n, \boldsymbol{p}] = 0. \quad (11)$$

To determine the first viscous correction δf, we work in a vicinity of the local rest frame $u^\mu = (1, u^i(\boldsymbol{x}, t))$, and substitute $f = n(\boldsymbol{p}, \boldsymbol{x}) + \delta f$ into Eq. (10) keeping terms first order in the spatial derivatives

$$\frac{p^i p^j}{E_p T} n_p (1 \pm n_p) \langle \partial_i u_j \rangle = -\mathcal{C}[\delta f, \boldsymbol{p}]. \qquad (12)$$

Here $\mathcal{C}[\delta f, \boldsymbol{p}]$ denotes the linearized collision operator, i.e., the collision operator expanded to first order in δf. In writing Eq. (12), we used ideal hydrodynamics and thermodynamic relations to rewrite time derivatives as spatial derivatives, and we neglected gradients proportional to $\partial_i u^i$ which are responsible for the bulk viscosity [27]. Equation (12) is an integral equation for δf which can be solved by various methods.

Since the first viscous correction is a scalar and must be proportional to the strains, the most general form for the viscous correction in the local rest frame can be parametrized by the function $\chi(p)$ as in Eq. (7). Close to equilibrium, the first viscous correction δf determines the strains

$$\pi^{ij} = -2\eta \langle \partial^i u^j \rangle = \int \frac{d^3 \boldsymbol{p}}{(2\pi)^3} \frac{p^i p^j}{E_{\boldsymbol{p}}} \delta f, \qquad (13)$$

which ultimately yields a relation between the shear viscosity and the viscous correction $\chi(p)$, that is,

$$\eta = \frac{1}{15} \int \frac{d^3 \boldsymbol{p}}{(2\pi)^3} \frac{p^2}{E_{\boldsymbol{p}}} n_p (1 \pm n_p) \chi(p). \qquad (14)$$

This is the only general constraint on the functional form of the viscous distribution function. To proceed further we must specify completely the form of the linearized collision operator, which we will do in the context of various model theories.

A. Simplest model: Relaxation time approximation

The simplest model (really a cartoon) for the collision operator is the relaxation time approximation

$$\mathrm{C}[\delta f, \boldsymbol{p}] = \frac{f(\boldsymbol{p}) - f_0(\boldsymbol{p})}{\tau_R(E_p)}, \qquad (15)$$

where τ_R is the momentum-dependent relaxation time to be specified. Substituting this form for the collision operator into Eq. (12), and working in a Boltzmann approximation $n_p(1 \pm n_p) \to n_p$ yields the following form for δf:

$$\delta f = -\frac{\tau_R(E_p)}{T E_{\boldsymbol{p}}} n_p p^i p^j \langle \partial_i u_j \rangle. \qquad (16)$$

Note, however, that the relaxation time is in general energy dependent. In different theories, $\tau_R(E_p)$ might show different functional dependence on E_p. Without details about the dynamics of the theory in question, we can only parametrize the viscous correction. Here we will discuss a massless classical gas, where $n_p = e^{-p/T}$, and we parametrize the relaxation time (or the distribution function) with a simple power law

$$\delta f(p) = -n_p \chi(\tilde{p}) \hat{p}^i \hat{p}^j \langle \partial_i u_j \rangle,$$
$$\chi(\tilde{p}) = C(\alpha) \tilde{p}^{2-\alpha}. \qquad (17)$$

The constant, $C(\alpha)$, is determined through Eq. (14):

$$C(\alpha) = \frac{120\eta}{(\epsilon + \mathcal{P}) \Gamma(6 - \alpha)}. \qquad (18)$$

There are two limiting cases for the functional form of the relaxation time approximation: $\alpha = 0$ and $\alpha = 1$. The momentum dependence of the relaxation time in these extreme cases is

$$\tau_R(p) \propto \begin{cases} p & \alpha = 0 \text{ (quadratic } Ansatz\text{),} \\ \text{const} & \alpha = 1 \text{ (linear } Ansatz\text{).} \end{cases} \qquad (19)$$

Most theories will lie between these two extreme limits.[3] Loosely speaking, if the energy loss of high-momentum particles grows linearly with momentum, $\frac{dp}{dt} \propto p$, one expects a relaxation time independent of momentum, $\tau_R \propto p^0$. On the other hand, if the energy loss approaches a constant $\frac{dp}{dt} \propto$ const, the relaxation time will grow with the particle momentum $\tau_R \propto p$.

Figure 2 shows the elliptic flow computed using these two functional forms for the first viscous correction. It is important to emphasize that shear viscosity is the same in both cases. Examining these figures, we see that the integrated elliptic flow

---

[3]There are exceptions to this rule. For instance, in a gas of Goldstone bosons far below the symmetry-breaking scale, one expects $\alpha = 2$, since the cross section grows rapidly with energy, $\sigma \sim E^2 / \Lambda^4$.
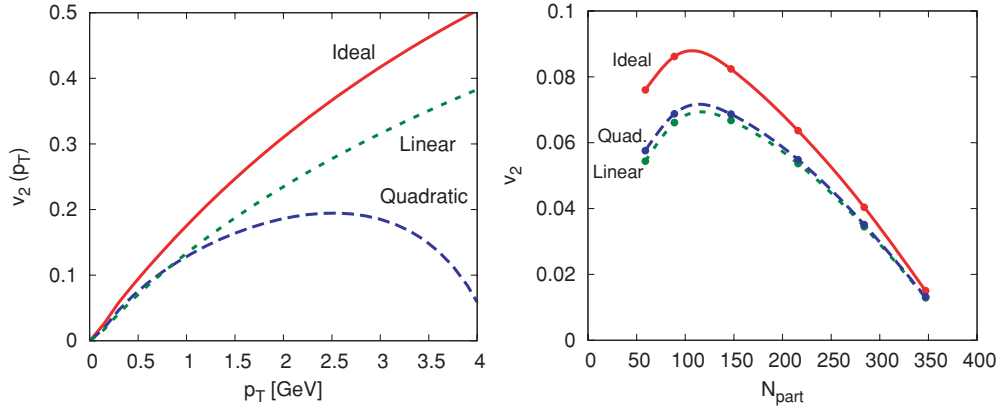
FIG. 2. (Color online) Left: $v_2(p_T)$ using the linear or quadratic *Ansätze* for the distribution function. Right: Integrated v_2 vs centrality showing independence from the precise form of the viscous correction. Run parameters can be found in Fig. 1.

is largely insensitive to the functional form of the first viscous correction. This is because the integrated v_2 is primarily determined by the hydrodynamic variables e, u^μ, $\pi^{\mu\nu}$ which are independent of the functional dependence of the relaxation time [27]. The differential elliptic flow $v_2(p_T)$ is sensitive to the rate of equilibration especially above $p_T \simeq 1.2$ GeV.

B. Scalar $\lambda\phi^4$ theory

Scalar field theory has been described at length by Jeon [28], who rigorously derived the Boltzmann equation and its collision kernel and then solved for $\chi(\tilde{p})$ numerically. But if we make the approximation of Boltzmann statistics, we can actually solve for δf in closed form.

First the nonlinear Boltzmann equation with Bose-Einstein statistics is

$$C[f, \boldsymbol{p}] = \int_{k,p',k'} \Gamma_{pk \to p'k'}[f_p f_k (1 + f_{p'})(1 + f_{k'}) - f_{p'} f_{k'}(1 + f_p)(1 + f_k)], \quad (20)$$

where the transition rate (including a final-state symmetry factor) is

$$\Gamma_{pk \to p'k'} = \frac{1}{2} \frac{|\mathcal{M}|^2}{(2E_p)(2E_k)(2E_{p'})(2E_{k'})} \times (2\pi)^4 \delta^4(P + K - P' - K'), \quad (21)$$

and we have used the traditional short hand, $\int_p = \int \frac{d^3 \boldsymbol{p}}{(2\pi)^3}$. After linearizing, $f(\boldsymbol{p}) \to n_p + n_p(1 \pm n_p)\chi(\boldsymbol{p})$ the linearized collision integral is

$$\frac{p^i p^j}{T E_p} \langle \partial_i u_j \rangle = \int_{k,p',k'} \Gamma_{pk \to p'k'} n_p n_k (1 + n_{p'})(1 + n_{k'}) \times [\chi(\boldsymbol{p}) + \chi(\boldsymbol{k}) - \chi(\boldsymbol{p'}) - \chi(\boldsymbol{k'})]. \quad (22)$$

At this point we will make the Boltzmann assumption by neglecting the stimulation factors, $(1 + n_p) \to 1$, and using $n_p = e^{-p/T}$. Then we will try a solution of the form

$$\chi(\boldsymbol{p}) = C p^i p^j \langle \partial_i u_j \rangle / T^3, \quad (23)$$

i.e., assuming that $\chi(\tilde{p}) \propto \tilde{p}^2$ or $\alpha = 0$. Substituting this form into the integral equation [Eqs. (12) and (22)] and performing the integrals yields (see Appendix B)

$$\langle \partial_i u_j \rangle \frac{p_i p_j}{T} = C \langle \partial_i u_j \rangle p_i p_j \frac{\lambda^2}{384\pi^3 T}. \quad (24)$$

Thus, taking $C = 384\pi^3/\lambda^2$, the quadratic form in Eq. (23) has provided an exact solution to the linearized integral equation. The viscosity is $\eta = 1536\pi T^3/\lambda^2$ in a Boltzmann approximation.

Physically, this happens because of the form of the scattering cross section. Since $\sigma \propto \lambda^2/s$ and $s \propto p$, the cross section scales as the inverse of the particle's energy. The typical scattering is nearly randomizing, but high-energy particles undergo fewer scatterings than low-energy ones.

This example from scalar field theory, together with the example of momentum diffusion (see Sec. III C 1 below), is the reason that most people assume the quadratic *Ansatz*, $\chi(p) \propto p^2$, should hold.

C. Weakly coupled pure-glue QCD

In this section, we will use the Boltzmann equation for pure-glue QCD in three approximation schemes to calculate the first viscous correction. First we will consider a leading $\log(T/m_D)$ approximation where the dynamics can be summarized by a Fokker-Planck equation which describes the momentum diffusion of quasiparticles. In this limit, we will find that the viscous correction is quadratic at large momentum, $\chi(p) \propto p^2$. Next we will consider the QCD Boltzmann equation but consider only $2 \to 2$ collisions and neglect collinear radiation. In this limit, we will find that the viscous correction at large momentum behaves as $\chi(p) \propto p^2/\log(p)$. Finally, we will also include collinear radiation in the Boltzmann equation as is necessary in a complete leading-order treatment [29,30]. We will find that collinear radiation controls the relaxation of the high-momentum modes, and asymptotically we have $\chi(p) \propto p^{3/2}$, where the coefficient of proportionality is set by the rate of transverse momentum broadening, $\hat{q}$. The impatient

reader may skip to Sec. III C4, which summarizes the results of these three approximation schemes.

1. Momentum diffusion in a leading log treatment

In a leading log approximation, $\log(T/m_D)$ is considered a large number and the dynamics describes soft Coulomb scattering. Each soft collision involves a small momentum transfer of order $q \sim gT$, but these collisions happen relatively frequently at a rate of $\sim g^2 T$ (neglecting logarithms). Thus a typical particle with momentum T will diffuse in momentum space and equilibrate on a time scale of $\sim g^4 T$. The resulting Boltzmann equation linearized around equilibrium can be written as a Fokker-Planck equation [31,32]

$$\partial_t \delta f + v_{\boldsymbol{p}} \cdot \partial_x \delta f = T \mu \frac{\partial}{\partial p^i}\left[n_p(1+n_p)\frac{\partial}{\partial p^i}\left(\frac{\delta f(\boldsymbol{p})}{n_p(1+n_p)}\right)\right]$$
$$+ \text{gain terms}, \qquad (25)$$

where μ is the drag coefficient of a high-momentum gluon in this approximation scheme [33,34]

$$\frac{d\boldsymbol{p}}{dt} = -\mu \hat{\boldsymbol{p}}, \quad \text{with} \quad \mu = \frac{g^4 C_A^2}{24\pi} T^2 \ln\left(\frac{T}{m_D}\right). \quad (26)$$

The precise form of the gain terms has been given in Refs. [31,32], but only involves the $\ell = 0, 1$ spherical harmonic components of $\delta f(\boldsymbol{p})$, i.e., $\int d\Omega_{\boldsymbol{p}} \delta f(\boldsymbol{p})$ and $\int d\Omega_{\boldsymbol{p}} \hat{\boldsymbol{p}} \delta f(\boldsymbol{p})$. In the hydrodynamic limit considered here, $\delta f(\boldsymbol{p})$ is proportional to a traceless rank 2 tensor $(\hat{p}^i \hat{p}^j - \delta^{ij}/3)$ and these gain terms vanish. Substituting the form of Eq. (7) into Eq. (25) leads to the following equation for $\chi(p)$:

$$n_p(1+n_p)\frac{p}{T} = T\mu n_p(1+n_p)\left[-\frac{d^2}{dp^2} + \left(\frac{1+2n_p}{T} - \frac{2}{p}\right)\frac{d}{dp}\right.$$
$$\left. + \frac{6}{p^2}\right]\chi(p). \qquad (27)$$

We are not aware of a closed form solution to this equation, but we can find a solution for $\chi(p)$ at large momentum. Making the approximation $1 + 2n_p \approx 1$, we find that

$$\chi(p) = \frac{p^2}{2T\mu} \qquad (28)$$

solves this equation. This is the well-known *quadratic Ansatz*.

2. Boltzmann equation with $2 \to 2$ collisions

We next will consider the QCD Boltzmann equation, but we will neglect collinear radiation. We emphasize that this is not a consistent approximation scheme. Nevertheless, it illustrates clearly the relative roles of hard collisions and inelastic processes in determining the functional form of $\chi(p)$ in the relevant subasymptotic regime.

The linearized Boltzmann equation is the same as Eq. (22), but the squared matrix element is

$$|\mathcal{M}|^2 = 8g^4 C_A^2 \left(3 - \frac{ut}{s^2} - \frac{us}{t^2} - \frac{ts}{u^2}\right), \qquad (29)$$

which describes $2 \to 2$ gluon scattering after summing over all spins and colors and dividing by the gluon degeneracy factor $2d_A$. These matrix elements must be dynamically screened using hard thermal loops. A procedure which is consistent at leading order (where the Debye mass is small) but which makes a reasonable estimate when the Debye mass is not small has also been described in Ref. [35], and we can follow exactly the numerical procedure of that reference to find $\chi(\tilde{p})$.[4] We can also study the asymptotic behavior more directly. At asymptotically large momentum where $\log(\tilde{p})$ may be considered large, Appendix B shows that

$$\chi(p) \propto \frac{p^2}{\log(p/T)}. \qquad (30)$$

The constant in front of the log is related to $\langle dE/dt\rangle_p$, the rate of collisional energy loss of a gluon with momentum p,

$$\chi(p) = \frac{p^2}{2T\langle dE/dt\rangle_p}. \qquad (31)$$

In a leading $\ln(p/T)$ approximation, the loss rate is [34,36]

$$\left\langle \frac{dE}{dt}\right\rangle_p = \frac{g^4 C_A^2}{48\pi} T^2 \ln\left(\frac{p}{T}\right), \qquad (32)$$

as is rederived in Appendix B. The above asymptotic form agrees well with the numerical solution of the Boltzmann equation.

3. A leading-order treatment at asymptotically large momenta

Early calculations of the shear viscosity in pure-glue QCD found $\chi(\tilde{p}) \propto \tilde{p}^2$, that is, $\alpha = 0$ [37,38]. However, this is because they were leading-log treatments, which reduced to momentum diffusion discussed above. It was realized in Refs. [29,30] that inelastic number changing processes are only suppressed by a log, but are enhanced at large energy E by a factor of $(E/T)^{1/2}$ and dominate equilibration for $E/T > \log(1/g)$.

This should not be a surprise. After all, if we think about "equilibration" (energy loss) in QED, we find that although the leading-order mechanism for the energy loss of a high-energy electron is ionization (elastic scattering), bremsstrahlung actually dominates the loss rate. This is the case because in bremsstrahlung the energy lost per scattering can scale with the incident energy, rather than being incident energy independent as is the case with ionization. As a result, the penetration depth of an electromagnetic shower scales only logarithmically with the incident energy, i.e., the relaxation time is constant up to logs, $\tau_R \propto E^0$. If the same behavior occurred in QCD, we would expect the linear *Ansatz* to hold, $\alpha = 1$.

The current understanding of energy loss in perturbative QCD is that the high-energy behavior lies between these extremes. High-energy particles in a QCD plasma lose energy predominantly by inelastic gluon radiation, and the time scale for energy loss is short compared to the time scale for

---

[4]Some minor technical difficulties are discussed in the next section.

momentum diffusion ("jet broadening"). In particular, Baier *et al.* showed that for $E \gg T$ the rate of (inelastic) energy loss scales with the incident energy as $dE/dt \propto E^{1/2}$, with the half-integer power arising from the Landau-Pomeranchuk-Migdal (LPM) suppression [39,40]. This implies a "relaxation time" which scales as $\tau_R \sim E/(dE/dt) \propto E^{1/2}$, and therefore $\alpha = 1/2$ [35]. Let us see how this emerges in the behavior of pure-glue QCD.

The point is that the Boltzmann equation for a gluon plasma possesses both an elastic scattering term and an inelastic effective $1 \to 2$ scattering term,

$$\partial_t f + v_{\mathbf{p}} \cdot \partial_{\mathbf{x}} f = -\mathcal{C}^{2 \leftrightarrow 2}[f] - \mathcal{C}^{1 \leftrightarrow 2}[f]. \qquad (33)$$

This equation was first solved at leading order in α_s by Arnold, Moore, and Yaffe to determine the shear viscosity [35]. Their approach involved writing a multiparameter *Ansatz* for $\chi(\tilde{p})$ in terms of a basis of test functions. While the determination of η improves quadratically with the test function basis, the determination of $\chi(\tilde{p})$ improves only linearly. Therefore to get good accuracy out to $p = 15T$ requires the use of a large basis of functions. We find a basis of eight functions is sufficient, and the $\tilde{p}^{3/2}$ behavior is already clear with such a basis.[5]

We can also directly establish the asymptotic form of the solution. At asymptotically high momentum, near-collinear bremsstrahlung dominates the equilibration of gluons. We therefore look at the Boltzmann equation including only $1 \to 2$ splittings,

$$\partial_t f + v_{\mathbf{p}} \cdot \partial_{\mathbf{x}} f = -\mathcal{C}^{1 \to 2}[f]. \qquad (34)$$

The relevant collision integral for near-collinear joining and splitting of gluons at leading order in α_s was worked out in [41]

$$\mathcal{C}^{1 \to 2} = \frac{(2\pi)^3}{2|\mathbf{p}|^2 \nu_g} \int_0^\infty dp' dk' \delta(|\mathbf{p}| - p' - k') \gamma(\mathbf{p}; p', k')$$
$$\times [f_{\mathbf{p}}(1 + f_{p'})(1 + f_{k'}) - f_{p'} f_{k'}(1 + f_{\mathbf{p}})], \qquad (35)$$

and is given in terms of the splitting function for $g \to gg$. In general, this splitting function involves the solution of an integral equation which includes the LPM effect. However, in the *deep* LPM regime [42] where $\ln^{-1}(\tilde{p})$ can be treated as small, the following leading log result for the splitting function can be obtained

$$\gamma_{gg}^g(p : xp, (1-x)p) = \frac{4\alpha_s C_A d_A}{(2\pi)^4} \sqrt{3p\hat{q}} \frac{[1 - x(1-x)]^{5/2}}{[x(1-x)]^{3/2}}. \qquad (36)$$

The above splitting function contains the transport parameter $\hat{q}$, which characterizes the typical transverse momentum squared transferred to the particle per unit length. With the above splitting function, we show in Appendix C that the solution of the off-equilibrium distribution function at

---

[5] In fact we find greatly improved convergence of the large-momentum behavior, both in terms of basis set size and numerical integration precision, by changing the test functions of Ref. [35] to a set which shows the correct large-momentum asymptotic behavior by multiplying $\phi_{2...N}$ defined in Eq. (2.32) of the reference by $\tilde{p}^{-1/2}$.
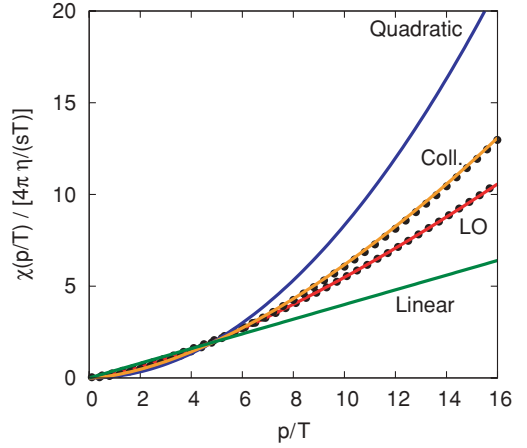

FIG. 3. (Color online) The points are from the numerical solution of the Boltzmann equation for pure glue at leading order (LO) and without $1 \leftrightarrow 2$ processes (i.e., collisional energy loss only). The lines are $\chi \propto p^{2-\alpha}$ for $\alpha = 2$, 1.6, 1.38, and 1, going from top to bottom.

asymptotically large momentum is

$$\chi_g(p) \approx \frac{0.7}{\alpha_s T \sqrt{\hat{q}}} p^{3/2}. \qquad (37)$$

4. Summary of weakly coupled pure-glue QCD

Let us now summarize some of the main features of the off-equilibrium dynamics of pure-glue QCD at weak coupling. In the previous three sections, we looked at the behavior of the off-equilibrium correction for pure-glue QCD in various approximation schemes, deriving asymptotic behavior in each case. These asymptotics are listed later in Table I. In this section, we wish to focus on the phenomenologically more interesting region where the equilibrating parton has intermediate energies ($p \sim 10T$). In this case, one must resort to numerical solutions of the Boltzmann equation, which we present in Fig. 3.

To summarize Fig. 3, we will discuss the curves from top to bottom starting with the "Quadratic" curve. In the leading $\log(T/m_D)$ approximation, the linearized Boltzmann equation simplifies to a differential equation, Eq. (27). The numerical solution to this has been worked out in Refs. [31,32,38] and is well described for all momenta by the asymptotic quadratic form, $\chi = p^2/2T\mu$. The numerical result will be presented in a forthcoming work [32], and for now we show the quadratic result as the solid blue line. Next we considered QCD with the $2 \to 2$ gluon scattering matrix element at leading order. The agreement between the asymptotics derived in the previous section and the numerical solution can be found in Appendix B. At intermediate momentum, we show the numerical solution of the Boltzmann equation without inelastic processes as the data points under the curve labeled "Coll." The solid curve is the result of a power-law fit at intermediate momentum, $\chi \propto p^{1.6}$. In the leading order (LO) treatment when bremsstrahlung is included, we find further equilibration of the gluons, and our numerical results are reasonably described by the fit,
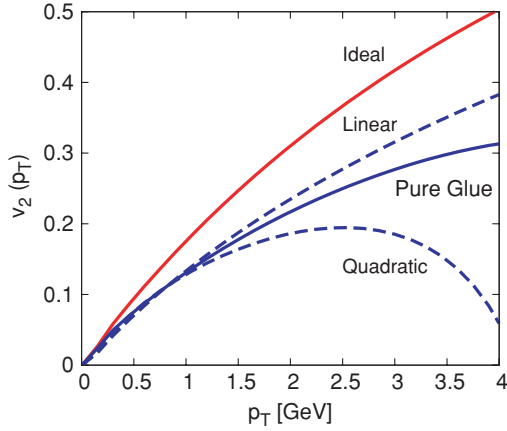
FIG. 4. (Color online) $v_2(p_T)$ for a perturbative gluon gas at leading order. The linear and quadratic *Ansätze* are shown for comparison. Run parameters can be found in Fig. 1.
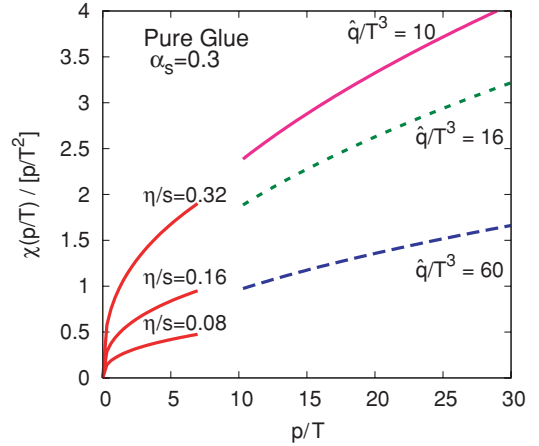

FIG. 5. (Color online) Curves at *lower* momentum are $\chi(p/T)$ for a perturbative gluon gas at leading order for three values of the nonperturbative parameter η/s. The curves at *higher* momentum show the asymptotic forms of χ for three values of the non-perturbative parameter $\hat{q}$. There must be a consistency between η/s and $\hat{q}$ in order that the curves merge at intermediate momentum.

$\chi \propto p^{1.38}$. Finally, the linear *Ansatz* is also shown in Fig. 3 for comparison.

One can now ask how the observed $\chi \propto p^{1.38}$ of pure glue at leading order will affect the viscous corrections to elliptic flow. First of all, as we have already shown, the integrated v_2 will change marginally. The differential v_2, on the other hand, will be largely affected at higher p_T. This result is shown in Fig. 4 along with the quadratic and linear *Ansätze* for comparison.

The above considerations have shown that the relaxation of the high-energy tail of the distribution is largely controlled by energy loss. The low- and intermediate-momentum regions are constrained by the shear viscosity via Eq. (14). The *strength* of the off-equilibrium correction is controlled by two nonperturbative parameters: η at low momentum and $\hat{q}$ at high momentum. This is clearly seen by looking at the forms of χ we have found for pure-glue QCD at leading order:

$$\chi(p) = \begin{cases} \frac{2.84\eta}{sT} \tilde{p}^{1.38} & 5 \lesssim \tilde{p} \lesssim 10, \\ \frac{0.7}{\alpha_s T \sqrt{\hat{q}}} p^{1.5} & \ln^{-1}(\tilde{p}) \ll 1. \end{cases} \quad (38)$$

In Fig. 5, we show plots of χ for various choices of the nonperturbative parameters η/s and $\hat{q}/T^3$. The main point to take away is the need for consistency between η and $\hat{q}$ such that the low- and high-momentum regions of χ can merge smoothly into one another. The three values of $\hat{q}/T^3 = 10, 16, 60$ we have chosen reproduce the experimentally observed R_{AA} [43] when convoluted with the higher twist [44], AMY [29,31,45], and ASW [39,40,46] energy loss models, respectively. It appears to be difficult to reconcile the discontinuity of χ between the lowest shear viscosity $\eta/s = 0.08$ and smallest value of $\hat{q}$ used in modeling heavy-ion collisions.

D. Hadron gas

One might also ask what scattering behavior is expected at lower temperatures, in a hadron gas. How do the highest energy hadrons equilibrate, as a function of hadron energy? A complete study requires understanding the energy-dependent hadron-hadron cross section, which has nontrivial energy dependence and must be determined from experiment. However,

we should be able to say something about the high-momentum behavior.

In hadron-hadron scattering, the inelastic branching fraction rises with increasing s, dominating the cross section for kinetic energies well above $\Lambda_{\rm QCD}$. Since generically no daughter in an inelastic collision carries more than half the energy of the initial high p particle, we can take scatterings to be momentum randomizing (the relaxation time approximation is sensible), especially for the highest energy hadrons. The relaxation time is then controlled by the scattering rate, $\tau_R \sim n\sigma$, with n the hadron number density and σ an averaged total hadronic cross section. So what is the behavior of the total hadronic cross section? At low momenta, it is complicated by resonances, but at large momenta there is universally a rising total cross section. Therefore the relaxation time $\tau_R(E)$ should naively involve a small or zero power of E, that is, $\alpha \sim 1$ is expected, at least for the very high energy tail.[6] Certainly we do not expect $\alpha = 0$. However, any more detailed discussion must be either model or data driven and lies outside the scope of this paper.

IV. MULTICOMPONENT PLASMAS

The plasmas just considered are treated as single-component type, in the sense that all degrees of freedom are related to each other by symmetries (polarizations by parity, colors by gauge invariance). The quark-gluon plasma is a multicomponent plasma. Treating m_s as small and m_c as large, the three light quark types behave the same, but the gluons behave differently from the quarks. Similarly, the hadronic plasma present at lower temperatures contains both baryons and mesons, each of several types. The different components generically have different departures from equilibrium, that is, $\chi_{\rm quark} \neq \chi_{\rm gluon}$, which would manifest as different viscous

---

[6]Froissart behavior $\sigma \propto \ln^2(s)$ suggests $\tau_R \propto \ln^{-2}(p)$.
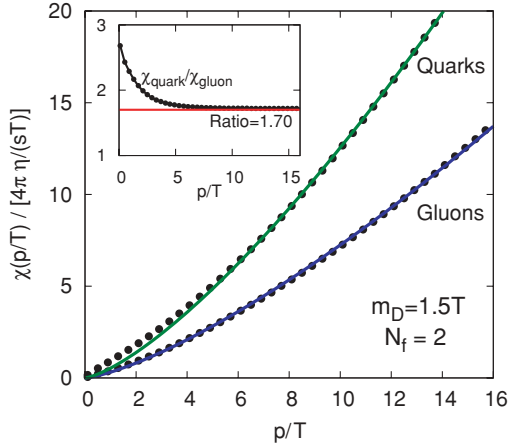
FIG. 6. (Color online) Off-equilibrium correction for the case of a perturbative two-flavor QGP evaluated at leading order. The inset figure shows the ratio of the quark to gluon correction which asymptotically approaches $\chi_{\text{quark}}/\chi_{\text{gluon}} \approx 1.7$.

corrections to their p_T spectra. In particular, we will argue that faster equilibration for baryons than for mesons can give a simple explanation for the "constituent quark scaling" [6–8] observed in $v_2(p_T)$ for mesons and baryons, without invoking any model of coalescence.

A. Quark-gluon plasma

We now consider a two-component gas of quarks and gluons and label the distribution functions with subscripts q and g, respectively:

$$\delta f_g(p) = -n_p(1 + n_p)\chi_g(\tilde{p})\hat{p}^i\hat{p}^j\langle\partial_i u_j\rangle,$$
$$\delta f_q(p) = -n_p(1 - n_p)\chi_q(\tilde{p})\hat{p}^i\hat{p}^j\langle\partial_i u_j\rangle. \quad (39)$$

For use in hydrodynamic simulations, we will again fit the off-equilibrium component of the quarks' and gluons' distribution function to the following power law:

$$\chi_g(\tilde{p}) = C_g(\alpha_g)\tilde{p}^{2-\alpha_g},$$
$$\chi_q(\tilde{p}) = C_q(\alpha_q)\tilde{p}^{2-\alpha_q}. \quad (40)$$

The results of the numerical solution of the Boltzmann equation for the two-component case are shown as points in Fig. 6. The solid curves are the results of the fit done at intermediate momentum ($5 \leqslant \tilde{p} \leqslant 15$) with the result $\alpha_q \approx \alpha_g \approx 0.62$.

To solve for the two constants (C_q and C_g), we need two constraints. The first constraint relates the coefficients $C_{q,g}$ to the shear viscosity,

$$\eta = \frac{1}{15}\sum_{a=q,g} v_a C_a \int \frac{d^3 p}{(2\pi)^3} p^{3-\alpha_a} n_p(1 \pm n_p). \quad (41)$$

The sum is over quarks and gluons with degeneracies $v_g = 2d_A = 16$ and $v_q = 4d_f N_f = 24$. The second constraint comes from fixing the ratio of χ_q/χ_g to the numerical solution of the Boltzmann equation. This ratio is shown in Fig. 6, and at large enough momentum ($\tilde{p} \gtrsim 5$), we find

$$\frac{\chi_q}{\chi_g} \approx 1.70. \quad (42)$$

The explicit computation of the two coefficients ($C_{q,g}$) in terms of the above ratio and η/s is worked out in Appendix D.

In Fig. 7, we show the elliptic flow of quarks and gluons. Note the larger suppression for quarks as the gluons are forced into equilibrium much quicker. This quicker relaxation cannot simply be explained by naively assuming Casimir scaling, $\chi_q/\chi_g \approx C_A/C_F = 2.25$. Instead this ratio involves a playoff between the faster equilibration rate of gluons and the tendency of identity changing processes $q\bar{q} \leftrightarrow gg$, $q \leftrightarrow qg$, $g \leftrightarrow q\bar{q}$ to balance disequilibrium between the quarks and gluons. This ratio is evaluated analytically at asymptotically large momentum in Appendix C.

The distinct quark and gluon elliptic flow is completely due to the different viscous corrections, which in turn are related to the different relaxation rates of quarks and gluons. Let us note that if we scale both the v_2 and p_T of gluons by 3 and of quarks by 2, the result is a "universal curve" as shown in the right plot of Fig. 7. The observed scaling was completely accidental, but it led us to consider the possibility of finding similar scaling behavior in a system of mesons and baryons
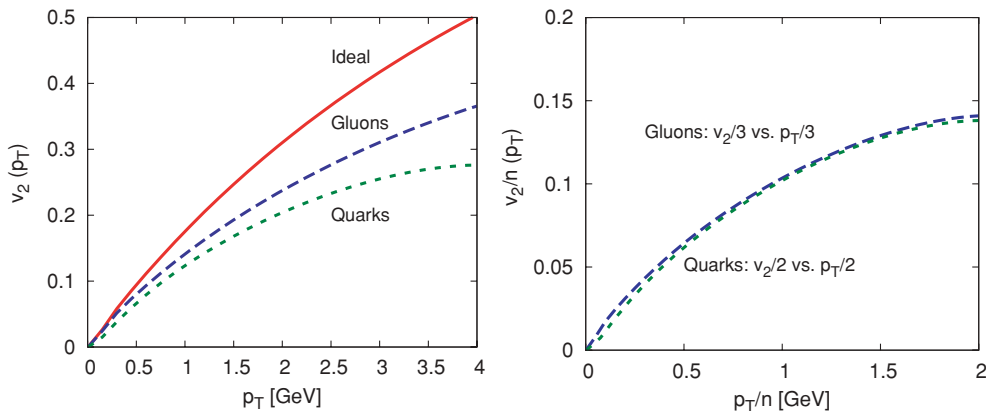

FIG. 7. (Color online) Left: Elliptic flow of quarks and gluons. Right: Both v_2 and p_T scaled by $n = 3, 2$ for gluons and quarks, respectively. Run parameters can be found in Fig. 1.

due to differences in the relaxation rates. This is discussed in detail in the next section.

B. Two-component meson-baryon gas

The QCD matter immediately before freeze-out is certainly not a weakly coupled quark-gluon plasma, but it might be described as a hadron (resonance) gas. Just as for the quarks and gluons, there is no reason to think that the mesons and baryons should show the same efficiency in equilibrating. But rather than claim a specific model for the partially equilibrated state of such a system, we will just do some phenomenology to see how different thermalization rates could affect the observed species-dependent elliptic flow behavior. To study the hydrodynamics of this system, we switch from the ideal-gas equation of state to a lattice motivated [47] one. Further details of the simulation are presented in Appendix A.

We consider a meson-baryon gas whereby mesons and baryons have the off-equilibrium corrections f_m and f_b, respectively,

$$\delta f_m(p) = -n_p(1 + n_p)\chi_m(\tilde{p})\hat{p}^i\hat{p}^j\langle\partial_i u_j\rangle,$$
$$\delta f_b(p) = -n_p(1 - n_p)\chi_b(\tilde{p})\hat{p}^i\hat{p}^j\langle\partial_i u_j\rangle. \tag{43}$$

We assume both species have the same power-law correction to spectra,

$$\chi_m(\tilde{p}) = C_m(\alpha)\tilde{p}^{2-\alpha},$$
$$\chi_b(\tilde{p}) = C_b(\alpha)\tilde{p}^{2-\alpha}, \tag{44}$$

but we allow for different coefficients (C_m/C_b) which we will choose in order to give reasonable agreement with data. For simplicity, we will consider two different *Ansätze*: quadratic ($\alpha = 0$) and radiative ($\alpha = 0.5$), and take the following ratios which, as we will show, fit the data rather well:

$$\frac{C_m}{C_b} = \begin{cases} 1.6 & \text{quadratic,} \\ 1.4 & \text{radiative.} \end{cases} \tag{45}$$

Finally, the numerical values of the coefficients can be identified with the shear viscosity through

$$\eta = \frac{1}{15}\sum_{a=\pi, K, \ldots} v_a C_{m/b}\int\frac{d^3p}{(2\pi)^3 E_a}p^{4-\alpha}n(E_a)[1 \pm n(E_a)], \tag{46}$$

where the sum extends over all mesons and baryons having $M \leqslant 1.8$ and 2.0 GeV, respectively. This choice reproduces the lattice parametrization of the equation of state below $T = 160$ MeV. We find the following values for the coefficients at our freeze-out temperature of $T = 150$ MeV:

$$\left.\begin{array}{l} C_m = 1.053 \\ C_b = 0.658 \end{array}\right\}\left(\frac{\eta}{s}\right) \text{ quadratic,} \tag{47}$$

$$\left.\begin{array}{l} C_m = 2.661 \\ C_b = 1.901 \end{array}\right\}\left(\frac{\eta}{s}\right) \text{ radiative.} \tag{48}$$

Before computing particle spectra, we would like to make an aside about the way elliptic flow is computed. By definition, $v_2(p_T)$ is given by

$$v_2(p_T) \equiv \frac{\int d\phi \cos(2\phi)(dN + \delta dN)}{\int d\phi (dN + \delta dN)}, \tag{49}$$

where dN is short for $dN/dp_T d\phi$ and δdN is the first viscous correction to this. In the above expression, the viscous correction to the phase-space distribution, δdN, occurs both in the numerator as well as in the normalization from the denominator. Since we have restricted the viscous correction to be linear in gradients of field quantities, we should therefore require that v_2 be computed to the same order. We therefore expand the denominator

$$v_2 \approx \frac{\int d\phi \cos(2\phi)\,dN + \delta dN}{\int d\phi\,dN} - \frac{\int d\phi\,\delta dN\int d\phi\cos(2\phi)\,dN}{(\int d\phi\,dN)^2}, \tag{50}$$

so the expression retains terms to first order in δf only. In the following we will show both the expanded and unexpanded expressions for v_2, shading the region between the two results in order to give an estimate for the uncertainty in the gradient expansion. The upper limit of the band corresponds to Eq. (49), while the lower limit is Eq. (50). In figures where the uncertainty band is omitted, the plotted curve corresponds to Eq. (49).

Let us now discuss how the different *Ansätze* fare with the experimental data. We have chosen $\eta/s = 0.16$ in order to give reasonable agreement with the data in the transverse momentum range $1 \leqslant p_T \leqslant 2$ GeV. The $v_2(p_T)$ spectra for K_S and Λ are presented in Fig. 8 using either the radiative ($p_T^{1.5}$) or quadratic (p_T^2) *Ansatz*. For $p_T \lesssim 2$ GeV, we find good agreement between the viscous hydrodynamic results and the data. If hadronic rescattering was included, the low-momentum component of the Λ v_2 would be pushed out toward higher p_T giving better agreement with the data. Above 2–3 GeV, large differences between the radiative and quadratic *Ansätze* are realized. We must warn that at higher p_T one cannot make a direct comparison with data, since a larger fraction of the yield will come from fragmenting partons, which have not been included. In addition, the hydrodynamic description starts to break down at larger p_T. Regardless, one must keep in mind that for large enough momentum (i.e., $p_T \gtrsim 2$–3 GeV), the two *Ansätze* used here are clearly discernible and the choice of *Ansatz* could in principle lead to differences in the extracted viscosity.

We would now like to investigate whether we observe meson to baryon scaling, similar to the accidental quark to gluon scaling we found from first principles earlier. For clarity, we again present the above results with mesons and baryons on the same figure. This is shown for both radiative and quadratic *Ansätze* in Fig. 9. The figures show the corresponding results with both v_2 and p_T rescaled by the number of constituent quarks. The scaling of the data is the well-known phenomenon of constituent quark scaling. We find that viscous hydrodynamics reproduces this "universal curve" as well. This is due to the difference in relaxation rates between mesons and baryons, which was treated as a free parameter. The possible microscopic origin of this ratio is discussed further in Sec. V.
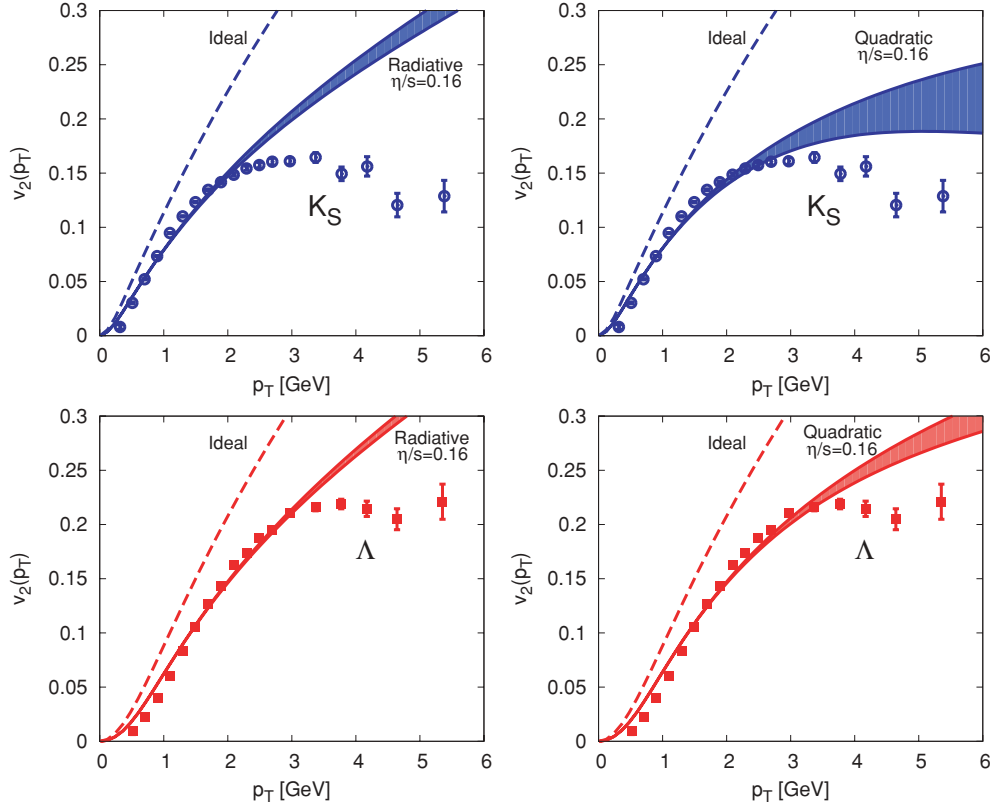
FIG. 8. (Color online) Elliptic flow of K_S mesons and Λ baryons from viscous hydrodynamics with radiative or quadratic *Ansätze*. The run parameters are $\eta/s = 0.16$, $T_{\text{frzout}} = 150$ MeV, and lattice EOS. Further details are in Appendix A. The data are from the STAR Collaboration [6].

We should also point out that this relaxation time scaling is fairly robust to changes in the equation of state. While changing the equation of state will clearly affect the $\eta = 0$ behavior, these changes will only modestly modify the viscous correction to the distribution functions. The qualitative feature that species with smaller relaxation times have a stronger elliptic flow is borne out by Fig. 7 (a quark-gluon plasma equation of state) and Fig. 9 (a lattice equation of state). Further study of the equation of state is left to future work.

V. SUMMARY AND DISCUSSION

In this work we have presented a systematic study of the first viscous correction to the thermal distribution function. All simulations of viscous hydrodynamics so far have used the quadratic *Ansatz*

$$\chi(p) \propto p^2, \qquad (51)$$

but this is only an educated guess.

First we studied the form of δf [or $\chi(p)$] in a momentum-dependent relaxation time approximation and derived the simple formula

$$\chi(p) = \tau_R(p) \frac{p}{T}. \qquad (52)$$

Examining this formula, we considered two special cases $\tau_R \propto p$ (where the equilibration time is proportional to energy) and $\tau_R = \text{const}$ (where the equilibration time is independent

of energy). These give rise to quadratic [$\chi(p) \propto p^2$] and linear [$\chi(p) \propto p$] dependence on momentum, as is summarized in Table I. We expect that, provided QCD is describable in terms of quasiparticles, the first viscous correction should lie between these cases. Figure 2 compares these two extreme limits for the functional form of the viscous correction. It is important to emphasize that the two simulations have precisely the same shear viscosity. Comparing our results for the elliptic flow in these two theories, we see that the integrated elliptic flow v_2 is largely determined by the shear viscosity, while differential quantities such as $v_2(p_T)$ at high p_T depend on the equilibration rates at high momentum. The integrated elliptic flow is determined to a large extent by the hydrodynamic variables e, u^μ, $\pi^{\mu\nu}$. (An explicit formula relating v_2 to e, u^μ, and $\pi^{\mu\nu}$ is given in Ref. [27] which in turn was motivated by earlier observations [15,17,50,51].)

The quadratic *Ansatz* is valid only for fairly specialized theories. For instance, examining Table I, we see that scalar theories follow this *Ansatz*. The reason is that the cross section falls as $1/s$, so higher energy particles see a more transparent medium and equilibrate more slowly.

For different reasons, the quadratic *Ansatz* is also valid in a soft scattering approximation to high-temperature QCD (see row 4 of Table I). In this limit, which treats $\log(T/m_D)$ as an expansion parameter, soft gT collisions lead to the momentum diffusion and drag of hard gluons. If the momentum diffusion is independent of particle energy and the drag is constant, we get the quadratic *Ansatz*. If the momentum diffusion increases
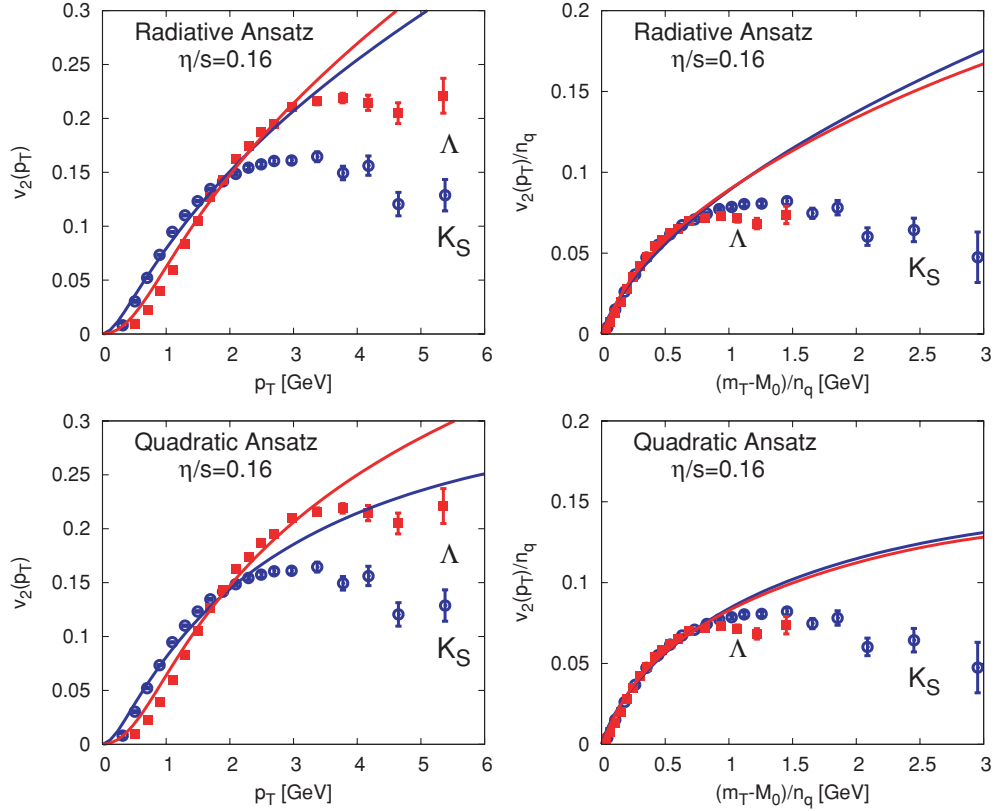
FIG. 9. (Color online) Left: v_2 of K_S and Λ. Right: Constituent quark scaling of $v_2(p_T)$. Run parameters can be found in Fig. 8. The data are from the STAR Collaboration [6] and are plotted in $(M_T - m)/n$ as suggested by the PHENIX Collaboration [7]. (Recent PHENIX data [48,49] clearly deviate from constituent quark scaling above $(M_T - m)/n \simeq 1$ GeV.)

logarithmically with particle energy, we find a logarithmic correction to this *Ansatz* (see row 5 of Table I). A formula which summarizes the asymptotic form of both of these cases is

$$\chi(p) = \frac{p^2}{2T \langle dE/dt \rangle_p}, \quad (53)$$

where $\langle dE/dt \rangle_p$ is the rate of energy loss of a particle with momentum p [see Eq. (26) and Eq. (32) for explicit formulas in certain limits].

However, the effect of bremsstrahlung completely changes this picture. A naive (Bethe-Heitler) treatment of radiative energy loss would lead to a relaxation rate independent of momentum; but when including the LPM effect, the viscous

correction behaves asymptotically as

$$\chi(p) = 0.7 \frac{p^{3/2}}{\alpha_s \sqrt{\hat{q}}}. \quad (54)$$

This formula is summarized in row 6 of Table I and provides a concrete connection between viscous corrections and radiative energy loss, which is further explored in Fig. 5 and surrounding text.

From a phenomenological perspective, the LPM effect is not entirely dominant, and collisions are important in the relevant momentum range. A phenomenological fit to numerical results for the first viscous correction, including both collisions and collinear radiation without making the strict

TABLE I. Summary of the functional dependence of the departure from equilibrium on the theory and approximation considered.

Model	Physics	Formula
Relaxation time, $\tau_R \propto p$	Relaxation time grows with particle momentum.	$\chi(p) \propto p^2$
Relaxation time, $\tau_R = $ const	Relaxation time independent of momentum.	$\chi(p) \propto p$
Scalar theory	Randomizing collisions which happen rarely.	$\chi(p) \propto p^2$
QCD soft scatt.	Soft $q \sim gT$ collisions lead to a random walk of hard particles.	$\chi(p) \propto p^2$
QCD hard satt.	Hard $q \sim \sqrt{pT}$ collisions lead to a random walk of hard particles.	$\chi(p) \propto \dfrac{p^2}{\log(p/T)}$
QCD rad. energy loss	Radiative energy controls the approach to equilibrium. In the LPM regime, $\hat{q}$ controls the radiation rate.	$\chi(p) \propto \dfrac{p^{3/2}}{\alpha_s \sqrt{\hat{q}}}$

LPM approximation, shows that the first viscous correction is reasonably well described by the following phenomenological form:

$$\chi(p) \simeq C \tilde{p}^{1.38}. \quad (55)$$

Figure 4 compares this functional form to the linear and quadratic *Ansätze* motivated by the relaxation time approximation. We see that the general expectation from high-temperature QCD is that in the relevant momentum range, the first viscous correction is slightly closer to the linear than to the quadratic *Ansatz*.

We next studied a two-component plasma starting with a two-component plasma of quarks and gluons. Since the relaxation rates of the quarks and gluons are not the same, the two components do not have the same distribution function. At high momentum, an analysis of collinear splittings $g \rightarrow gg$, $g \rightarrow q\bar{q}$, $q \rightarrow gq$ shows that both the quark and gluon distribution behave as $p^{3/2}$. However, the ratio of the quark and gluon viscous corrections approaches a constant:

$$\frac{\chi_q}{\chi_g} \approx 1.70. \quad (56)$$

The constant is determined by the ratio of Casimirs $C_A/C_F = 9/4$ and the dynamics of the QCD splitting functions. It also depends weakly on the number of quark flavors, and we have quoted the two-flavor case.

Motivated by this example, we have postulated that the baryon and meson components of the medium have different equilibration rates. Indeed, there is no reason to expect that these species would equilibrate at the same rate. Then we fitted (by eye) the ratio of relaxation rates to reproduce the baryon and meson elliptic flows. If the ratio of relaxation times is

$$\frac{\chi_m}{\chi_b} \simeq 1.5, \quad (57)$$

meaning that baryons relax to equilibrium 1.5 times faster than mesons, then the resulting viscous hydrodynamic calculation effortlessly reproduces the universal constituent quark scaling curve. Physically what is happening is that in ideal hydrodynamics, the baryons and mesons have approximately the same elliptic flow, which is approximately described by a linear rise in m_T. The viscous correction then dictates that the baryons will follow this ideal trend 1.5 times farther than the mesons. Although it is not obvious from the data shown in Fig. 9, the data do not show scaling above $(m_T - M_o)/n_q \simeq 1$ GeV, i.e., the last Λ point is a fluctuation upward. (This is seen quite clearly in recent PHENIX data [48,49].) It is interesting that the data also deviate from hydrodynamic predictions above this point.

It is tempting to speculate as to the microscopic origin of the factor of 1.5. The baryons and mesons in the 2–3 GeV region are produced in the complex transition region where the energy density decreases from 1.2 to 0.5 GeV/fm^3. In this range, the temperature decreases by only $\Delta T \simeq 20$ MeV. However, the hydrodynamic simulations evolve this complicated region for a significant period of time, $\tau \simeq 4 \leftrightarrow 6.5$ fm, and the hadronic currents are built up over this time period. The interactions are probably quite inelastic and are not easily classified as hadronic or partonic in nature. The additive quark model was used to describe high-energy total cross sections which are similarly inelastic [52]. It predicts the ratio of high-energy nucleon-nucleon to pion-nucleon (as well as pion-nucleon to pion-pion) cross sections to be 3/2 in reasonable agreement with the experimental ratio. Perhaps similar physics is responsible for the different baryon and meson elliptic flows. In fact, the splitting of the baryonic and mesonic elliptic flows was predicted at least qualitatively by UrQMD, which implements the additive quark model [53]. On the other hand, the factor of 1.5 in the relative relaxation times could be simply a combination of dynamical and group theoretical factors of accidental significance.

In summary, a species-dependent relaxation time provides a coherent and physically transparent explanation for the complicated trends observed in the elliptic flow data measured at the BNL Relativistic Heavy Ion Collider.

APPENDIX A: DETAILS OF HYDRODYNAMIC DESCRIPTION

The initial condition of hydrodynamic evolution is set by a Glauber model, and the energy density is proportional to the number of binary collisions. More specifically, we take

$$\epsilon(\tau_0 = 1 \text{ fm}, x, y) = E_{\text{BC}} \times \frac{n_{\text{coll}}(b, x, y)}{\sigma_{NN}}, \quad (A1)$$

where $E_{\text{BC}} = 22.735$ is the energy per binary collision and $\sigma_{NN} = 40$ mb is the inelastic nucleon-nucleon cross section.

In this work, we will use the following evolution equation for π^{ij}:

$$\dot{\pi}^{ij} = -\frac{1}{\tau_\pi}(\pi^{ij} - \eta\sigma^{ij}) - 2\pi^{ij}\partial_k u^k + \pi_{k(i}\omega^k_{j)} + \frac{1}{\eta}\pi_{k\langle i}\pi^k_{j\rangle}, \quad (A2)$$

which is identical to the stress tensor used in Ref. [17]. Other possibilities are also possible [54] which will not change the results of this work on a qualitative level. In the above expression, $\omega_{ij} \equiv \partial_j u_i - \partial_i u_j$ is the vorticity and $\tau_\pi = 3\eta/(4p)$. There is one technical detail that warrants discussion. At large transverse distances, the viscous pressure tends to become larger than the ideal pressure, and the equations become unstable. It is therefore necessary to cut off our auxiliary tensor when it becomes large. More precisely,

we take

$$\pi^{ij} \rightarrow \frac{\pi^{ij}}{1 + \kappa \mathrm{Tr} \pi^2}, \tag{A3}$$

where $\mathrm{Tr}\pi^2 = \sqrt{\pi_{11}^2 + \pi_{22}^2 + \pi_{33}^2}$ and $\kappa \approx 0.1/(\alpha p)$.

In the first part of this paper, we consider an ideal-gas equation of state, $p = 1/3\epsilon$. For a two-flavor QGP the ideal Stefan-Boltzmann gas gives $\epsilon = 12.71 T^4$, which roughly corresponds to the ϵ/T^4 relation found on the lattice. (For the highest temperatures in the simulation, it is above this value; and for the lowest temperatures in the simulation, it is this value). We have decided to use the same ϵ/T^4 ratio for both the gluon gas and quark + glue simulations in order to get the fairest possible phenomenological estimate for the size of the viscous corrections in a realistic heavy-ion event.

For simulations using the ideal-gas EOS, the freeze-out contour is taken at constant $\epsilon_{\mathrm{frzout}} = 0.6$ GeV/fm^3 corresponding to a temperature of 140 MeV. The default impact parameter is 7.6 fm, and the shear viscosity to entropy ratio is $\eta/s = 0.08$.

In the second part of this paper, where we compute spectra of a meson-baryon gas, we use a lattice-motivated equation of state [47]. In this case, the freeze-out surface is set by $\epsilon_{\mathrm{frzout}} = 0.24$ GeV/fm^3 corresponding to a temperature of 150 MeV. We use a default impact parameter of 6.8 fm corresponding to a centrality class of 10–40% and a shear viscosity to entropy ratio of $\eta/s = 0.16$.

APPENDIX B: COLLISION INTEGRALS

In this section, we will give the details leading to Eq. (24) for a scalar theory and Eq. (31) for pure glue.

1. Scalar theory

Our starting point is Eq. (22). Substituting the form specified in Eq. (23) into this equation yields in a Boltzmann approximation

$$
\begin{aligned}
\frac{\langle \partial_i u_j \rangle p_i p_j}{T} & \frac{e^{-p/T}}{p} \\
= & \frac{C \langle \partial^\mu u^\nu \rangle}{T^3} \frac{e^{-p/T}}{2p} \int \frac{d^3 k}{(2\pi)^3 2k} e^{-k/T} \frac{\lambda^2}{2} \\
& \times \int \frac{d^4 P' d^4 K'}{(2\pi)^2} \delta(P'^2)\delta(K'^2)\delta^4[(P+K) - P' - K'] \\
& \times (P_\mu P_\nu + K_\mu K_\nu - P'_\mu P'_\nu - K'_\mu K'_\nu),
\end{aligned} \tag{B1}
$$

where $\langle \partial^\mu u^\nu \rangle$ is the Lorentz invariant extension[7] of $\langle \partial^i u^j \rangle$. The integrals over P' and K' are Lorentz covariant and can be performed by standard tricks; the $(P_\mu P_\nu + K_\mu K_\nu)$ term can be

---

[7]Specifically, defining the projector onto the local rest frame $\Delta^{\mu\nu} = g^{\mu\nu} + u^\mu u^\nu$, we have

$$\langle \partial^\mu u^\nu \rangle = \tfrac{1}{2} \Delta^{\mu\rho} \Delta^{\nu\sigma} (\partial_\rho u_\sigma + \partial_\sigma u_\rho - \tfrac{2}{3} \Delta_{\rho\sigma} \partial_\beta u^\beta).$$

In the local rest frame implicit here, we have $\langle \partial^0 u^\mu \rangle = 0$ and $\langle \partial^\mu u^\nu \rangle = \langle \partial^i u^j \rangle$ for $\mu, \nu = 1 \ldots 3$.

factored out, leading to $\int_{P', K'} = 1/8\pi$, while the integral over $P'_\mu P'_\nu + K'_\mu K'_\nu$ must return a rank-2 tensor depending only on $(P + K)_\mu$. There are only two such tensors, and contraction with $g^{\mu\nu}$ and $(P + K)^\mu (P + K)^\nu$ establishes that

$$
\begin{aligned}
\int \frac{d^4 P' d^4 K'}{(2\pi)^2} & \delta(P'^2)\delta(K'^2) \\
& \times \delta^4[(P+K) - P' - K'](P'_\mu P'_\nu + K'_\mu K'_\nu) \\
= & \frac{1}{48\pi}[4(P + K)_\mu (P + K)_\nu - (P + K)^2 g_{\mu\nu}]. \tag{B2}
\end{aligned}
$$

The integral equation becomes

$$
\begin{aligned}
\frac{\langle \partial_i u_j \rangle p_i p_j}{T} = & \frac{C \langle \partial_i u_j \rangle \lambda^2}{32\pi T^3} \int \frac{d^3 k}{(2\pi)^3 2k} e^{-k/T} \\
& \times \left(p_i p_j + k_i k_j - \frac{2}{3}(p + k)_i (p + k)_j \right), \tag{B3}
\end{aligned}
$$

where we used that $\langle \partial^\mu u^\nu \rangle$ is traceless, so $\langle \partial^\mu u^\nu \rangle g_{\mu\nu} = 0$. Performing the k angular integration in the plasma frame, the $p_i k_j$ terms integrate to zero; so does the $k_i k_j$ term, because $\langle \partial_i u_j \rangle$ is traceless. Performing the trivial radial integration, we find Eq. (24).

2. Pure glue

Our goal here is to derive Eqs. (31) and (32). Our starting point is the collision integral Eq. (21) with matrix elements given by Eq. (29)

$$
\begin{aligned}
\frac{p^i p^j}{T E_p} \langle \partial_i u_j \rangle = & \int_{p'kk'} n_p n_k (1 + n_{k'})(1 + n_{p'}) \Gamma_{pk \rightarrow p'k'} \\
& \times [\chi(\boldsymbol{p}) + \chi(\boldsymbol{k}) - \chi(\boldsymbol{p'}) - \chi(\boldsymbol{k'})]. \tag{B4}
\end{aligned}
$$

Using the definition, $\chi(\boldsymbol{p}) = \chi(p)(\hat{p}^i \hat{p}^j - \delta^{ij}/3)\langle \partial_i u_j \rangle$, one can pull out the common factor, $\langle \partial_i u_j \rangle$. The remaining integral on the right-hand side (called I^{ij}) must have the form $I^{ij} = I(p)(\hat{p}^i \hat{p}^j - \delta^{ij}/3)$ since this is the only symmetric traceless tensor which can be constructed out of $\boldsymbol{p}$ and δ^{ij}. Straightforward analysis then shows that

$$
\begin{aligned}
\frac{p n_p (1 + n_p)}{T} = & \int_{p'kk'} n_p n_k (1 + n_{k'})(1 + n_{p'}) \Gamma_{pk \rightarrow p'k'} \\
& \times [\chi(p) + \chi(k) P_2(\cos\theta_{\boldsymbol{pk}}) - \chi(p') P_2(\cos\theta_{\boldsymbol{pp'}}) \\
& - \chi(k') P_2(\cos\theta_{\boldsymbol{pk'}})], \tag{B5}
\end{aligned}
$$

where, for instance,

$$P_2(\cos\theta_{\boldsymbol{kp}}) = \frac{3}{2}\left(\hat{p}^i \hat{p}^j - \frac{1}{3}\delta^{ij}\right)\left(\hat{k}^i \hat{k}^j - \frac{1}{3}\delta^{ij}\right), \tag{B6}$$

is the second Legendre polynomial.

We will evaluate this integral in a leading $\log(p/T)$ approximation. Asymptotically, the momenta p and p' are large, while k and k' are of order the temperature.[8] In this limit,

---

[8]We will discuss the region of phase space where $t = -(P' - P)^2$ is small. Since the particles are identical, there is also an equal contribution where $u = -(K' - P)^2$ is small, i.e., when p and k'

we can make the Boltzmann approximation, $(1 + n_{p'}) \to 1$, and can treat p' as close to p. Specifically we take

$$\cos\theta_{pp'} = 1 + \frac{t}{2pp'} \simeq 1, \tag{B7}$$

and then write

$$\chi(p) - \chi(p') \simeq -\frac{\partial\chi}{\partial p}\omega. \tag{B8}$$

We also note that k and k' are close to T and therefore $\chi(k)$ and $\chi(k')$ are small. Then we can write Eq. (B6) as

$$\frac{p}{T} \simeq \frac{\partial\chi}{\partial p}\left\langle\frac{dE}{dt}\right\rangle_p, \tag{B9}$$

where the average energy loss rate for a particle with momentum p is

$$\left\langle\frac{dE}{dt}\right\rangle_p = -\int_{p'kk'}\Gamma_{pk\to p'k'}n_k(1 + n_{k'})\omega, \tag{B10}$$

i.e., the energy loss is the transition rate weighted with the energy transfer. The energy loss to leading $\log(p/T)$ has been determined by Bjorken [36] and Braaten and Thoma [34] and reads

$$\left\langle\frac{dE}{dt}\right\rangle_p \simeq \frac{g^4 C_A^2 T^2}{48\pi}\ln\left(\frac{p}{T}\right). \tag{B11}$$

One can verify that when terms suppressed by $\log(p/T)$ are dropped, we have

$$\chi(p) = \int_{\sim T}^{\sim p}\frac{p'}{T\langle dE/dt\rangle_{p'}}dp' \simeq \frac{1}{T\langle dE/dt\rangle_p}\frac{1}{2}p^2. \tag{B12}$$

In Fig. 10, a fit based on Eq. (B12) does a reasonable job in reproducing our $N_c = 3$ numerical results at high momentum.

For completeness, we will rederive Eq. (B11). To evaluate the phase-space integrals over $\Gamma_{pk\to p'k'}$, we use the "t-channel parametrization" of Ref. [35]. Following the logic that leads from (A.14) to (A.21) of that work, we write the phase space as

$$\int_{p'kk'}\Gamma_{pk\to p'k'}$$

$$= \frac{1}{(2\pi)^4 16p^2}\int_0^\infty dk\int_0^{2\pi}d\phi\int_{PS}dq\int_{PS}d\omega|\mathcal{M}|^2, \tag{B13}$$

where the momentum transfer is $\mathbf{q} = \mathbf{p}' - \mathbf{p} = \mathbf{k} - \mathbf{k}'$ and the energy transfer is $\omega = p' - p = k - k'$. The vector $\mathbf{q}$ is taken along the z axis and the vector $\mathbf{p}$ lies in the z-x plane. The angle ϕ is the azimuthal angle of $\mathbf{k}$ with respect to the z-x plane. The energy transfer and momentum transfer are restricted to the available phase space

$$0 < \frac{q+\omega}{2} < k, \tag{B14}$$

$$0 < \frac{q-\omega}{2} < p, \tag{B15}$$

which is also exhibited in Fig. 11.

---

are large and p' and k are of order T. Our original definition of the transition rate includes a $1/2$ symmetry factor for the identical particle final state. To ease the discussion in this section, we will simply drop the symmetry factor and neglect the u-channel contribution.
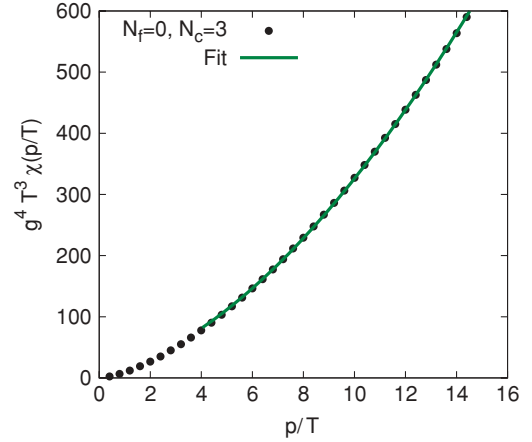

FIG. 10. (Color online) Off-equilibrium correction for the case of collisional energy loss. The points are from the numerical solution of the linearized Boltzmann equation, and the curve is the asymptotic form, Eq. (B12). Specifically the curve is a one-parameter fit to the $N_c = 3$ form, $(24\pi/9)\,\tilde{p}^2/\log(\tilde{p}/C)$, with fit parameter $C^{-1} = 1.3$.

Using the definitions of the kinematic variables, the Mandelstam invariants are

$$t = -(P' - P)^2 = q^2 - \omega^2, \tag{B16}$$

$$s = -(P + K)^2 = \frac{-t}{2q^2}[(p + p')(k + k') + q^2$$
$$- \cos\phi\sqrt{(4pp' + t)(4kk' + t)}], \tag{B17}$$

$$u = -t - s. \tag{B18}$$

To evaluate the collision integral, we are to substitute these expressions for the Mandelstam invariants into the matrix elements and perform the integrals over the phase space. Close inspection of the result of this procedure shows how $\log(p/T)$ comes about. First, the logarithm comes from integrating over the phase-space region where $\omega \simeq -q$ and $T \ll q \ll p$ as shown by the band in Fig. 11. Since the ω integral is over the interval $-q < \omega < -q + 2k$, the phase-space integral is approximately

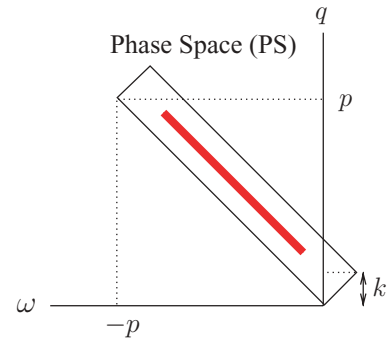$$\int_{PS}dq\int_{PS}d\omega \simeq 2k\int_{\sim T}^{\sim p}dq, \tag{B19}$$

FIG. 11. (Color online) Available phase space for the collision integrals in Eq. (B13). The band shows the dominant region of the integration in a leading $\log(p/T)$ approximation.

and we may neglect the stimulation factor, $(1 + n_{k'}) \simeq 1$. Second, only the highest powers of ω and q contribute to the ultraviolet logarithm. The ϕ integrated matrix element with these restrictions is

$$\int_0^{2\pi} d\phi \frac{-us}{t^2} \simeq \frac{2\pi p^2}{q^2}. \qquad (B20)$$

Then the total total transition rate is

$$\left\langle \frac{dE}{dt} \right\rangle_p = -\frac{1}{(2\pi)^4 16 p^2} \left(8 g^4 C_A^2\right) \int_0^\infty dk 2 k n_k$$

$$\times \int_{\sim T}^{\sim p} dq \frac{2\pi p^2}{q^2}(-q). \qquad (B21)$$

Performing the integral over k, we arrive at the result quoted in Eq. (B11).

APPENDIX C: VISCOUS DISTRIBUTION FUNCTION AND $\hat{q}$

In this appendix, we derive the form of the viscous distribution function for asymptotically large momenta. In doing this we will relate the high p_T tail of the distribution function with the energy loss parameter $\hat{q}$.

The starting point is the Boltzmann equation containing near-collinear splitting processes. We neglect $2 \leftrightarrow 2$ processes as these will be subleading at large momenta. Therefore,

$$\frac{p^\mu}{E_p} \partial_\mu f_a(\mathbf{x}, \mathbf{p}) = -\mathcal{C}_a^{1 \to 2}[f], \qquad (C1)$$

where

$$\mathcal{C}_a^{1 \to 2} = \frac{(2\pi)^3}{2|\mathbf{p}|^2 \nu_a} \int_0^\infty dp' dk' \delta(|\mathbf{p}| - p' - k') \gamma(\mathbf{p}; p', k')$$

$$\times [f_p(1 \pm f_{p'})(1 \pm f_{k'}) - f_{p'} f_{k'}(1 \pm f_p)]. \quad (C2)$$

In the above expression, f_a is the distribution function of species a. The degeneracy factor ν_a is 16 for gluons and 6 for quarks.

Now linearize the collision integral

$$\mathcal{C}^{1 \to 2} = \frac{(2\pi)^3}{2 p^2 \nu_g} \int_0^\infty dp' dk' \delta(p - p' - k') \gamma(p : p', k') n_p$$

$$\times (1 \pm n_{p'})(1 \pm n_{k'})[\chi_p - \chi_{p'} - \chi_{k'}]. \qquad (C3)$$

Doing the integral over k' and expanding out the left-hand side in the typical way, we get

$$\beta n_p (1 \pm n_p) \frac{p^2}{E_p} = -\frac{(2\pi)^3}{2 p \nu_a} \int_0^\infty dx \gamma(p : xp, (1-x)p) n_p$$

$$\times (1 \pm n_{xp})(1 \pm n_{(1-x)p})$$

$$\times [\chi_p - \chi_{xp} - \chi_{(1-x)p}]. \qquad (C4)$$

Then note at very high momentum,

$$\frac{(1 \pm n_{xp})(1 \pm n_{(1-x)p})}{1 \pm n_p} \to \Theta(1 - x). \qquad (C5)$$

Let us now consider a two-component plasma of quarks and gluons. Using the *Ansatz* $\chi_{q,g}(p) = C_{q,g} p^{2-\alpha}$ we are left with

$$\frac{p^2 \nu_g}{(2\pi)^3} = \frac{1}{2} p^{2-\alpha} \int_0^1 dx \gamma_{gg}^g(p : xp, (1-x)p)[C_g - C_g x^{2-\alpha} - C_g(1-x)^{2-\alpha}]$$

$$+ p^{2-\alpha} \int_0^1 dx \gamma_{q\bar{q}}^g(p : xp, (1-x)p)[C_g - C_q x^{2-\alpha} - C_q(1-x)^{2-\alpha}], \qquad (C6)$$

$$\frac{p^2 N_{fl} \nu_q}{(2\pi)^3} = p^{2-\alpha} \int_0^1 dx \gamma_{gq}^q(p : xp, (1-x)p)[C_q - C_g x^{2-\alpha} - C_q(1-x)^{2-\alpha}].$$

The splitting functions at leading log order are

$$\gamma_{gg}^g(p : xp, (1-x)p) = \frac{\sqrt{6} \alpha_s C_A d_A}{(2\pi)^4} \sqrt{p\hat{q}} \frac{\sqrt{C_A + C_A x^2 + C_A(1-x)^2}[1 + x^4 + (1-x)^4]}{[x(1-x)]^{3/2}},$$

$$\gamma_{q\bar{q}}^g(p : xp, (1-x)p) = \frac{\sqrt{6} \alpha_s C_F d_F N_{fl}}{(2\pi)^4} \sqrt{p\hat{q}} \frac{\sqrt{(2C_F - C_A) + C_A x^2 + C_A(1-x)^2}[x^2 + (1-x)^2]}{[x(1-x)]^{1/2}}, \qquad (C7)$$

$$\gamma_{gq}^q(p : xp, (1-x)p) = \frac{\sqrt{6} \alpha_s C_F d_F N_{fl}}{(2\pi)^4} \sqrt{p\hat{q}} \frac{\sqrt{C_A + (2C_F - C_A)x^2 + C_A(1-x)^2}[1 + (1-x)^2]}{x[x(1-x)]^{1/2}}.$$

The $p^{1/2}$ behavior here together with the $p^{2-\alpha}$ behavior explicitly on the right-hand side of Eq. (C6) must cancel the p^2 behavior on the left side of Eq. (C6). This fixes $2 = 2 - \alpha + 1/2$ or $\alpha = 1/2$, so $\chi(\tilde{p}) \propto \tilde{p}^{3/2}$. This proves the claim in the main text that the asymptotic behavior should be $\alpha = 1/2$.

For a gluon gas, we find

$$C_g^{-1} = \frac{C_A^{3/2} \alpha_s \sqrt{3\hat{q}}}{2\pi T} \int_0^1 \frac{[1 - x(1-x)]^{5/2}}{[x(1-x)]^{3/2}}$$

$$\times [1 - x^{3/2} - (1-x)^{3/2}] dx, \qquad (C8)$$

and

$$\chi_g = \frac{0.704778}{\alpha_s T \sqrt{\hat{q}}} p^{3/2}. \tag{C9}$$

For a two-flavor quark-gluon gas we find

$$\chi_g = \frac{0.759158}{\alpha_s T \sqrt{\hat{q}}} p^{3/2},$$
$$\chi_q = \frac{1.257913}{\alpha_s T \sqrt{\hat{q}}} p^{3/2}. \tag{C10}$$

The ratio is

$$\frac{\chi_q}{\chi_g} = 1.657, \tag{C11}$$

not too different from the ratio 1.7 we found by fitting. This ratio depends on N_{fl}. For one flavor, it is 1.702, for three flavors it is 1.618, and in the limit of infinite flavors it approaches 1.128. This diminishing ratio occurs because, at larger N_{fl}, more and more splitting processes are $g \leftrightarrow q\bar{q}$ and $q \leftrightarrow qg$, which equilibrate the numbers of quarks and gluons toward each other.

APPENDIX D: TWO-COMPONENT SYSTEM

In this appendix, we derive relationships between the off-equilibrium distribution function, χ, and the shear viscosity of a two-component system.

We consider a gas of bosons and fermions because it will have applications to a gas of quarks and gluons or a gas of mesons and baryons.

$$\delta f_f(p) = -v_f n_p (1 - n_p) \chi_f(p) \hat{p}^i \hat{p}^j \langle \partial_i u_j \rangle,$$
$$\delta f_b(p) = -v_b n_p (1 + n_p) \chi_b(p) \hat{p}^i \hat{p}^j \langle \partial_i u_j \rangle. \tag{D1}$$

The off-equilibrium correction χ takes the form

$$\chi_b(p) = C_b(T) p^{2-\alpha_b},$$
$$\chi_f(p) = C_f(T) p^{2-\alpha_f}. \tag{D2}$$

The goal is to find values of the coefficients C_b and C_f as a function of T and η/s.

First we define the partial viscosity of each species

$$\eta_f = \frac{v_f}{15} \int \frac{d^3 p}{(2\pi)^3} p \chi_f(p) n_p [1 - n_p],$$
$$\eta_b = \frac{v_b}{15} \int \frac{d^3 p}{(2\pi)^3} p \chi_b(p) n_p [1 + n_p], \tag{D3}$$

which will yield a total viscosity of

$$\eta = \eta_f + \eta_b. \tag{D4}$$

For massive particles the phase space integrals must be done numerically, but for massless particles, integrating Eq. (D3) yields

$$C_f(T) = \frac{7\pi^4 \eta_f}{6 s_f T^{3-\alpha_f} \Gamma(6 - \alpha_f) \zeta_-(5 - \alpha_f)},$$
$$C_b(T) = \frac{4\pi^4 \eta_b}{3 s_b T^{3-\alpha_b} \Gamma(6 - \alpha_b) \zeta(5 - \alpha_b)}, \tag{D5}$$

with $\zeta_-(x) = \sum_{n=1}^{\infty} (-1)^{n-1} n^{-x} = (1 - 2^{1-x})\zeta(x)$. Let us define $\mathcal{R}$ as the ratio of the partial viscosities,

$$\frac{\eta_f}{\eta_b} \equiv \mathcal{R}. \tag{D6}$$

Making use of the relations

$$\eta = \eta_f + \eta_b = (1 + \mathcal{R})\eta_b,$$
$$s = s_f + s_b = v_f \frac{7\pi^2}{180} + v_b \frac{2\pi^2}{45}, \tag{D7}$$

we find

$$C_f(T) = \left(\frac{1 + \frac{8v_b}{7v_f}}{1 + \frac{1}{\mathcal{R}}} \right) \frac{\eta}{s} \frac{7\pi^4}{6 T^{3-\alpha_f} \Gamma(6 - \alpha_f) \zeta_-(5 - \alpha_f)},$$
$$C_b(T) = \left(\frac{1 + \frac{7v_f}{8v_b}}{1 + \mathcal{R}} \right) \frac{\eta}{s} \frac{4\pi^4}{3 T^{3-\alpha_b} \Gamma(6 - \alpha_b) \zeta(5 - \alpha_b)}. \tag{D8}$$

[1] J. Adams *et al.* (STAR Collaboration), Nucl. Phys. A **757**, 102 (2005).
[2] K. Adcox *et al.* (PHENIX Collaboration), Nucl. Phys. A **757**, 184 (2005).
[3] B. B. Back *et al.*, Nucl. Phys. A **757**, 28 (2005).
[4] I. Arsene *et al.* (BRAHMS Collaboration), Nucl. Phys. A **757**, 1 (2005).
[5] T. Hirano and Y. Nara, Nucl. Phys. A **743**, 305 (2004); D. Teaney, J. Lauret, and E. V. Shuryak, Phys. Rev. Lett. **86** 4783 (2001); P. F. Kolb, P. Huovinen, U. W. Heinz, and H. Heiselberg, Phys. Lett. B **500**, 232 (2001); P. Huovinen, P. F. Kolb, U. W. Heinz, P. V. Ruuskanen, and S. A. Voloshin, *ibid.* **503**, 58 (2001); C. Nonaka and S. A. Bass, Phys. Rev. C **75**, 014902 (2007).
[6] B. I. Abelev *et al.* (STAR Collaboration), Phys. Rev. C **77**, 054901 (2008).
[7] A. Adare *et al.* (PHENIX Collaboration), Phys. Rev. Lett. **98**, 162301 (2007).
[8] See, for example, the recent review of coalescence and constituent quark scaling: P. Sorensen, arXiv:0905.0174 [nucl-ex].
[9] Z. w. Lin and C. M. Ko, Phys. Rev. C **65**, 034904 (2002).
[10] D. Molnar and S. A. Voloshin, Phys. Rev. Lett. **91**, 092301 (2003).
[11] V. Greco, C. M. Ko, and P. Levai, Phys. Rev. Lett. **90**, 202302 (2003).
[12] R. J. Fries, B. Muller, C. Nonaka, and S. A. Bass, Phys. Rev. Lett. **90**, 202303 (2003).
[13] R. Baier and P. Romatschke, Eur. Phys. J. C **51**, 677 (2007).
[14] P. Romatschke, Eur. Phys. J. C **52**, 203 (2007).
[15] P. Romatschke and U. Romatschke, Phys. Rev. Lett. **99**, 172301 (2007).
[16] H. Song and U. W. Heinz, Phys. Lett. B **658**, 279 (2008).
[17] K. Dusling and D. Teaney, Phys. Rev. C **77**, 034905 (2008).
[18] P. Huovinen and D. Molnar, Phys. Rev. C **79**, 014906 (2009).
[19] H. Song and U. W. Heinz, Phys. Rev. C **77**, 064901 (2008).

[20] P. Bozek, Phys. Rev. C **77**, 034911 (2008).

[21] W. A. Hiscock and L. Lindblom, Ann. Phys. (NY) **151**, 466 (1983).

[22] W. A. Hiscock and L. Lindblom, Phys. Rev. D **31**, 725 (1985).

[23] W. Israel, Ann. Phys. (NY) **100**, 310 (1976); W. Israel and J. M. Stewart, Phys. Lett. A **58**, 213 (1976).

[24] M. Grmela and H. C. Öttinger, Phys. Rev. E **56**, 6620 (1997); H. C. Öttinger and M. Grmela, *ibid.* **56**, 6633 (1997); H. C. Öttinger, *ibid.* **57**, 1416 (1998).

[25] H. C. Öttinger, Physica A **254**, 433 (1998).

[26] F. Cooper and G. Frye, Phys. Rev. D **10**, 186 (1974).

[27] See, for example, D. A. Teaney, arXiv:0905.2433 [nucl-th].

[28] S. Jeon, Phys. Rev. D **52**, 3591 (1995).

[29] P. Arnold, G. D. Moore, and L. G. Yaffe, J. High Energy Phys. 11 (2001) 057.

[30] P. Arnold, G. D. Moore, and L. G. Yaffe, J. High Energy Phys. 01 (2003) 030.

[31] P. Arnold, G. D. Moore, and L. G. Yaffe, J. High Energy Phys. 11 (2000) 001.

[32] J. Hong and D. Teaney (unpublished).

[33] M. H. Thoma and M. Gyulassy, Nucl. Phys. A **544**, 573C (1992).

[34] E. Braaten and M. H. Thoma, Phys. Rev. D **44**, 1298 (1991); **44**, R2625 (1991).

[35] P. Arnold, G. D. Moore, and L. G. Yaffe, J. High Energy Phys. 05 (2003) 051.

[36] J. D. Bjorken, FERMILAB-PUB-82-059-THY (unpublished).

[37] G. Baym, H. Monien, C. J. Pethick, and D. G. Ravenhall, Phys. Rev. Lett. **64**, 1867 (1990).

[38] H. Heiselberg, Phys. Rev. D **49**, 4739 (1994).

[39] R. Baier, Y. L. Dokshitzer, A. H. Mueller, S. Peigne, and D. Schiff, Nucl. Phys. B **483**, 291 (1997).

[40] R. Baier, Y. L. Dokshitzer, A. H. Mueller, S. Peigne, and D. Schiff, Nucl. Phys. B **484**, 265 (1997).

[41] P. Arnold, G. D. Moore, and L. G. Yaffe, J. High Energy Phys. 06 (2002) 030.

[42] P. Arnold and C. Dogan, Phys. Rev. D **78**, 065008 (2008).

[43] S. A. Bass, C. Gale, A. Majumder, C. Nonaka, G. Y. Qin, T. Renk, and J. Ruppert, Phys. Rev. C **79**, 024901 (2009).

[44] X. Guo and X. N. Wang, Phys. Rev. Lett. **85**, 3591 (2000); X. N. Wang and X. f. Guo, Nucl. Phys. A **696**, 788 (2001); B. W. Zhang and X. N. Wang, *ibid.* **720**, 429 (2003); A. Majumder, E. Wang, and X. N. Wang, Phys. Rev. Lett. **99**, 152301 (2007); A. Majumder and B. Muller, Phys. Rev. C **77**, 054903 (2008); A. Majumder, R. J. Fries, and B. Muller, *ibid.* **77**, 065209 (2008).

[45] S. Jeon and G. D. Moore, Phys. Rev. C **71**, 034901 (2005).

[46] B. G. Zakharov, JETP Lett. **63**, 952 (1996); **65**, 615 (1997); Phys. At. Nucl. **61**, 838 (1998); C. A. Salgado and U. A. Wiedemann, Phys. Rev. D **68**, 014008 (2003); U. A. Wiedemann, Nucl. Phys. B **582**, 409 (2000); **588**, 303 (2000); C. A. Salgado and U. A. Wiedemann, Phys. Rev. Lett. **89**, 092303 (2002); N. Armesto, C. A. Salgado, and U. A. Wiedemann, *ibid.* **94**, 022002 (2005).

[47] M. Laine and Y. Schroder, Phys. Rev. D **73**, 085009 (2006).

[48] Arkadij Taranenko for the PHENIX Collaboration, presented at Quark Matter 2009, Knoxville, TN, March 30–April 4, 2009.

[49] S. Huang (PHENIX Collaboration), J. Phys. G **36**, 064061 (2009).

[50] P. F. Kolb, J. Sollfrank, and U. Heinz, Phys. Rev. C **62**, 054909 (2000).

[51] J. Y. Ollitrault, Phys. Rev. D **46**, 229 (1992).

[52] E. M. Levin and L. L. Frankfurt, Pisma ZhETP **3**, 105 (1965); H. J. Lipkin and F. Sheck, Phys. Rev. Lett. **16**, 71 (1966).

[53] M. Bleicher and H. Stoecker, Phys. Lett. B **526**, 309 (2002).

[54] K. Dusling, Acta Phys. Pol. B **40**, 963 (2009).